THE JOURNAL OF BIOLOGICAL CHEMISTRY
Vol. 277, No. 48, Issue of November 29, pp. 45803–45810, 2002
Printed in U.S.A.

Targeted Lysosome Disruptive Elements for Improvement of Parenchymal Liver Cell-specific Gene Delivery*

Received for publication, April 11, 2002, and in revised form, August 29, 2002
Published, JBC Papers in Press, September 16, 2002, DOI 10.1074/jbc.M203510200

Sabine M. W. van Rossenberg‡§, Karen M. Sliedregt-Bol¶, Nico J. Meeuwenoord¶, Theo J. C. van Berkel‡, Jacques H. van Boom¶, Gijs A. van der Marel¶, and Erik A. L. Biessen‡

From the ‡Division of Biopharmaceutics, Leiden/Amsterdam Center for Drug Research and the ¶Leiden Institute of Chemistry, Gorlaeus Laboratories, Leiden University, P. O. Box 9502, 2300 RA Leiden, The Netherlands

The transfection ability of nonviral gene therapy vehicles is generally hampered by untimely lysosomal degradation of internalized DNA. In this study we describe the development of a targeted lysosome disruptive element to facilitate the escape of DNA from the lysosomal compartment, thus enhancing the transfection efficacy, in a cell-specific fashion. Two peptides (INF7 and JTS-1) were tested for their capacity to disrupt liposomes. In contrast to JTS-1, INF7 induced rapid cholesterol-independent leakage (EC_{50}, 1.3 μM). INF7 was therefore selected for coupling to a high affinity ligand for the asialoglycoprotein receptor (ASGPr), $K(GalNAc)_2$, to improve its uptake by parenchymal liver cells. Although the parent peptide disrupted both cholesterol-rich and -poor liposomes, the conjugate, INF7-$K(GalNAc)_2$, only induced leakage of cholesterol-poor liposomes. Given that endosomal membranes of eukaryotic cells contain <5% cholesterol, this implies that the conjugate will display a higher selectivity toward endosomal membranes. Although both INF7 and INF7-$K(GalNAc)_2$ were found to increase the transfection efficiency on polyplex-mediated gene transfer to parenchymal liver cells by 30-fold, only INF7-$K(GalNAc)_2$ appeared to do so in an ASGPr-specific manner. In mice, INF7-$K(GalNAc)_2$ was specifically targeted to the liver, whereas INF7 was distributed evenly over various organs. In summary, we have prepared a nontoxic cell-specific lysosome disruptive element that improves gene delivery to parenchymal liver cells via the ASGPr. Its high cell specificity and preference to lyse intracellular membranes make this conjugate a promising lead in hepatocyte-specific drug/gene delivery protocols.

The development of a viable nonviral gene delivery system continues to be an important theme in gene therapy (1). The packaging of DNA into compact particles, the cellular uptake, the endosomal escape, and unpacking of these particles as well as the subsequent transfer of DNA to the nucleus are considered important steps in this regard (2). A number of DNA-packaging compounds have been reported, including cationic lipids, polymers and/or peptides that were designed to self-assemble with DNA to form intermolecular complexes (3–8). Upon internalization, the packaged DNA is transported to the lysosome, which subsequently degrades its content, making lysosomal escape a key step in gene delivery. To facilitate the intracellular transport of the packaged DNA to the nucleus and thus to enhance the transfection capacity of the nonviral gene delivery vehicles, lysosome disruptive elements (LDEs)[1] have been successfully applied, including amphipathic peptides (9–16).

The majority of the amphipathic peptides are derived from viral elements that promote cellular entry and correct intracellular handling. Their membrane permeabilizing capacity generally depends on the lipid composition and the pH. Although they are random coil at pH 7.0, these peptides undergo a conformational change into an amphipathic α-helix at pH 5.0 and aggregate into multimeric clusters (11, 12). Subsequently, the clustered helical peptides associate with and/or penetrate endosomal membranes, thereby destabilizing the membrane. Apart from complete virus capsids and purified capsid proteins, hemagglutinin (HA)-derived peptides and synthetic analogs have also been shown to induce pH-sensitive membrane disruption, leading to improved transfection of DNA-polycation complexes *in vitro* (9, 17). Although several groups have studied the stimulatory effect of LDEs on nonviral gene transfer (18–20), the use of targeted LDEs, which concomitantly improve the cellular delivery of DNA and its translocation to the nucleus, is rather unexplored.

Previous studies have shown that coupling of a homing device to liposomes or a universal carrier leads to a higher uptake of liposome-encapsulated drugs by the target cell (6, 23–25). The same strategy was applied to generate a targeted LDE. Two fusogenic peptides, INF7, a 23-mer peptide from HA, and JTS-1, an artificial INF7 mimic designed for pH-sensitive helix formation, were studied (10, 21, 22). INF7, the most promising peptide in terms of cholesterol dependence and disruption kinetics, was equipped with a homing device for the asialoglycoprotein receptor (ASGPr), $K(GalNAc)_2$ (1, 9, 23–26) on parenchymal liver cells.

In this report, we show that the glycoconjugated peptide, INF7-$K(GalNAc)_2$, displays a high affinity for the ASGPr and

* This work was supported by Chemische Wetenschappen/Stichting Technische Wetenschappen Project 349-4779 and the Netherlands Heart Foundation Project M93 001. The costs of publication of this article were defrayed in part by the payment of page charges. This article must therefore be hereby marked "*advertisement*" in accordance with 18 U.S.C. Section 1734 solely to indicate this fact.

§ To whom correspondence should be addressed: Division of Biopharmaceutics, Leiden/Amsterdam Center for Drug Research, Gorlaeus Laboratories, Leiden University, P. O. Box 9502, 2300 RA Leiden, The Netherlands. Tel.: 31-71-527-6213; Fax: 31-71-527-6032; E-mail: rossenbe@lacdr.leidenuniv.nl.

[1] The abbreviations used are: LDE(s), lysosome disruptive element(s); ASGPr, asialoglycoprotein receptor; BHK, baby hamster kidney; Boc, *t*-butoxycarbonyl; BOP, benzotriazol-1-yloxy-tris(dimethylamino)phosphonium hexafluorophosphate; BSA, bovine serum albumin; CMV, cytomegalovirus; Fmoc, *N*-(9-fluorenyl)methoxycarbonyl; HA, hemagglutinin; HOBt, hydroxybenzotriazole; HPLC, high performance liquid chromatography; $K(GalNAc)_2$, di-N^{α},N^{ϵ}-(5-(2-acetamido-2-deoxy-β-D-galactopyranosyloxy)pentanomido) lysine; LC-MS, liquid chromatography-mass spectrometry; Luc, luciferase; MALDI, matrix-assisted laser desorption/ionization; MTT, 3-(4,5-dimethylthiazol-2-yl)-2,5-diphenyltetrazolium bromide; TOF, time-of-flight.

possesses high lytic activity in cholesterol-poor liposomes only, making it eminently suitable for targeted fusogenic activity in parenchymal cells. Moreover, INF7-K(GalNAc)$_2$, unlike the parental INF7, accumulates efficiently in the liver after *in vivo* administration and strongly improves the transfer of polyplexed genes to parenchymal liver cells in an ASGPr-dependent fashion.

EXPERIMENTAL PROCEDURES

Materials—Egg yolk phosphatidylcholine was purchased from Fluka (Buchs, Switzerland). Cholesterol (>99%), calcein, trypsin inhibitor (bovine origin), orosomucoid, Triton X-100, 3-(4,5-dimethylthiazol-2-yl)-2,5-diphenyltetrazolium bromide (MTT), and BSA were obtained from Sigma. Precipath L was from Roche Molecular Biochemicals. Sepharose G50 and G10 were from Amersham Biosciences. Agarose was from Eurogentec (Seraing, Belgium), and dimethyl sulfoxide was obtained from Baker. All solvents were of analytical grade. Dry solvents were stored over molecular sieves of 4 Å. Kieselgel 60 F_{254} plates were from Merck. Polyethylene glycol-PS resin was purchased from PerkinElmer Life Sciences. Fmoc amino acids were purchased from Nova Biochem (Bad Soden, Germany). K(GalNAc)$_2$ was synthesized as described by Valentijn *et al.* (26). KWKKK KKKKK AKY (K8) was kindly provided by A. van Keulen (Leiden University, Leiden, The Netherlands).

Analysis—For TLC analysis, compounds were visualized by charring with sulfuric acid/ethanol (1/4, v/v) or with a 0.3% solution of ninhydrine in acetic acid/1-butanol (3/100, v/v). Column chromatography was performed with Kieselgel 60, 230–400 mesh (Merck). ^{1}H NMR spectra (300 MHz) were recorded with a Bruker WM-300 spectrometer. Solid phase synthesis was performed on an ABI 433 peptide synthesizer. Products were analyzed with a Jasco HPLC system using a LiChrospher® 100 RP-18 column (Merck, 5 μm, 4.6 × 250 mm). Automated purification was performed using BIOCAD VISION. Electrospray mass spectra were recorded with a PerkinElmer SCIEX API 165 single quadrupole LC-MS instrument. Matrix-assisted laser desorption/ionization (MALDI) time-of-flight (TOF) mass spectrometry was performed on a PerkinElmer/PerSeptive Biosystems Voyager-DE-RP MALDI-TOF mass spectrometer.

Peptide Synthesis—JTS-1 (GLEEALLFLLESLWELLLEA) was a generous gift from Dr. Tagliaferri (Valentis, Inc., Burlingame, CA). INF-7 (GLFEAIEGFIENGWEGMIWDYG) was prepared by solid phase synthesis on an ABI 433 peptide synthesizer (Wang resin, loading (L) 0.64 mmol/g) analogous to the procedure described by Planck *et al.* (19). A 50-μmol scale synthesis was performed using Fmoc/*tertiary*-butyl or Fmoc/trityl-protected amino acids with a BOP/HOBt activation strategy. Deprotection and cleavage of the peptide from the resin in a solution of 95% trifluoroacetic acid, 2.5% H_2O, and 2.5% triisopropylsilane were followed by precipitation of the peptide in ether. The precipitated crude INF7 was analyzed by LC-MS using a reversed phase C18 column eluted with a CH_3CN gradient (5–50% CH_3CN) in ammonium bicarbonate buffer (10 mM NH_4HCO_3) followed by HPLC purification eluting with a 20–40% CH_3CN gradient in aqueous 10 mM NH_4HCO_3. The product fractions were combined, concentrated, and subsequently lyophilized twice. The purity of the product (99%) was monitored by analytical HPLC and analysis with MALDI-TOF spectrometry (molecular weight: calculated, 2589.1; found, 2612.2 $[M+Na]^+$). The spacer arm containing INF7 (GLFEAIEGFIENGWEGMIWDYGSGSCG) was prepared under essentially the same conditions. The cysteine-protected peptide was synthesized and isolated as described above. Reversed phase HPLC yielded a product of ~95% purity as was assessed by LC-MS (CH_3CN gradient in 10 mM NH_4Ac, molecular weight: 3012, found weight, 1507; $[M+2H]^{2+}$). The peptide was taken up in 40 mM dithiothreitol in NH_4HCO_3 buffer) for a period of 1.5 h during which the deprotection of the cysteine residue was monitored by LC-MS. The peptide was purified (see above) (98%) and analyzed by LC-MS (molecular weight: 2924; found, 1463 $[M+2H]^{2+}$).

Preparation of the glycoconjugated INF7 peptide (Fig. 1, INF7-K(GalNAc)$_2$) commenced with the synthesis of a divalent lysine-based cluster galactoside on commercially available polyethylene glycol-PS resin, prior to introduction of the INF7 peptide. To this end, FmocLys-(Boc)-OH was attached to commercially available polyethylene glycol-PS via a hydroxymethylbenzoic acid linker to obtain **1** (Scheme 1, L 0.19 mmol/g). Subsequently, the Boc group was removed from the lysine side chain using trifluoroacetic acid in dichloromethane and the ϵ-amine group coupled to BocLys(Boc)-OH in the presence of *O*-7-azabenzotriazol-1-yl)-*N*,*N*,*N*′,*N*′-tetramethyluroniumhexafluorophosphate/*n*,*n*-di-isopropylethylamine (HATU/DiPEA). Deprotection of the latter lysine residue with trifluoroacetic acid/dichloromethane resulted

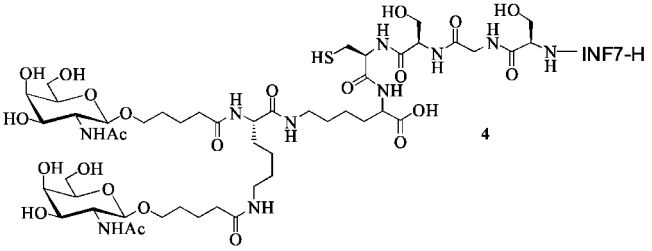

FIG. 1. **Synthetic structure of INF7-K(GalNAc)$_2$.**

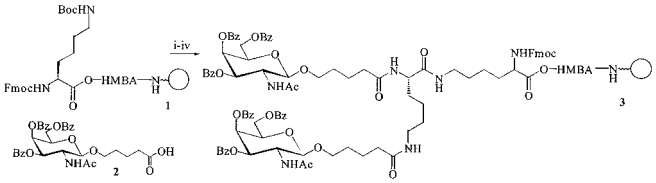

SCHEME 1. *i*, trifluoroacetic acid/DCM; *ii*, BocLys(Boc)-OH/HATU/DiPEA; *iii*, trifluoroacetic acid/DCM; *iv*, **2**, BOP/HOBt/DiPEA.

in two free amine groups thus permitting simultaneous introduction of both galactosamine-derived moieties **2** to give resin immobilized cluster galactoside **3** (L 0.10 mmol/g) (Scheme 1) (26). The obtained resin was treated with a 20% piperidine solution in *N*,*N*-dimethylformamide to remove the Fmoc protecting group, and the resulting free α-amino group was elongated with the SGSC amino acid spacer, followed by assembly of the INF-7 peptide as described above. Final deprotection and cleavage from the resin of the glycoconjugated INF7 **4** (Fig. 1) were performed as follows. Removal of the acid-labile tBu and Trt side chain protecting groups was achieved by treatment of the resin with trifluoroacetic acid, 2.5% H_2O, 2.5% triisopropylsilane, and 2.5% ethanedithiol (27), followed by washing with trifluoroacetic acid, 5% H_2O (twice), and H_2O (three times). Cleavage of the INF7 derivative **4** (Fig. 1) from the resin and simultaneous debenzoylation of the galactosamine moieties were achieved by uptake of the resin in an aqueous 0.4 M NaOH solution at 4 °C. The cysteine residue was deprotected using tributylphosphine in isopropyl alcohol. The obtained glycoconjugated peptide was analyzed by analytical HPLC (CH_3CN gradient in 10 mM NH_4HCO_3) and LC-MS (CH_3CN gradient in 10 mM NH_4Ac) assessed the presence of compound **4** (Fig. 1) as the main (~95%) product. Further purification by RP-HPLC using a CH_3CN gradient (5–50% CH_3CN) in 10 mM NH_4HCO_3 buffer gave conjugate **4** (Fig. 1) in an overall yield of 26% (99% pure). The product was analyzed by MALDI-TOF spectrometry (molecular weight: 3787.3 $[M+H]^+$ and 3809.3 $[M+Na]^+$, calculated, 3786.5) and lyophilized.

Leakage Assay—Phosphatidylcholine/cholesterol vesicles containing calcein were prepared by sonication. Briefly 100 mg/ml egg yolk phosphatidylcholine and cholesterol in methanol/chloroform (10 and 100 mg/ml) were dried under a stream of nitrogen. The lipid mixture was resuspended in sonication buffer (375 mM NaOH, 50 mM NaCl, pH 7.4) containing 100 mM calcein and sonicated with amplitude of 10 μm for 15 min (2.6% cholesterol) to 20 min (40% cholesterol) at 54 °C with a probe sonicator (Beun de Ronde, Abcoude, The Netherlands). Free calcein was separated from liposome-entrapped calcein by using a Sephadex G-50 column. Liposome size was measured routinely by photon correlation spectroscopy (Malvern Instruments, Malvern, UK) to exclude small and large particles. Measurements were performed at 27 °C and at a 90-degree angle. The average liposome size was 100 nm. The cholesterol content of the purified calcein laden liposomes was determined using a Roche enzymatic kit for cholesterol using Precipath L as a reference (28).

Calcein release was measured at 535 nm (λ_{ex} = 485 nm) using a fluorescence spectrophotometer (PerkinElmer Life Sciences). For the leakage assay the calcein-laden liposomes were diluted in citrate-buffered saline (200 mM NaCl, 20 mM sodium citrate), pH 7.0 or pH 5.0, and peptide was added at a concentration of 0–20 μM. Fluorescence was measured 0–60 min after the addition of the peptide. Complete lysis was achieved by adding Triton X-100 to a final concentration of 0.25%.

Leakage of Liposome-entrapped Trypsin Inhibitor—Liposomes were loaded with ^{125}I-trypsin inhibitor (molecular weight 20,000) as follows. Trypsin inhibitor was radioiodinated according to McFarlane (29) to a specific activity of 2340 dpm/ng (free $^{125}I < 5\%$). Liposomes were sonicated as described above in buffer (5 mM Hepes, 40 mM NaCl, pH 7.4) containing ^{125}I-trypsin inhibitor (33.8×10^6 dpm). Free ^{125}I-trypsin inhibitor was removed by density ultracentrifugation (40,000 rpm) for

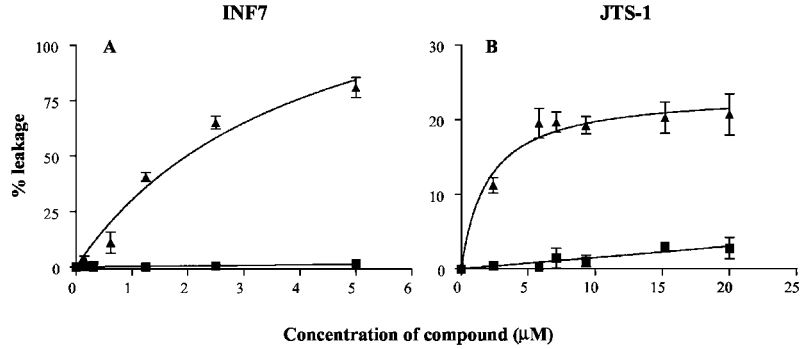

FIG. 2. **Liposome leakage assay of INF7 (*A*) and JTS-1 (*B*).** Calcein-laden 2.6% cholesterol containing liposomes were incubated at pH 7.0 (■) and pH 5.0 (▲) with various concentrations of peptide. Calcein release was quantified after 30 min of incubation as described under "Experimental Procedures." Data shown are the means ± S.D. of a triplicate determination.

16–18 h at 4 °C (30). Particles were characterized by size and cholesterol concentration.

For the leakage assay, the liposomes were diluted in citrate-buffered saline, pH 7.0 or pH 5.0. Fusogenic peptide was added to a concentration of 0–20 μM, and the amount of leakage was monitored by 0.75% w/w agarose gel electrophoresis in Tris/hippuric acid buffer, pH 8.8. Radioactivity was visualized using the PhophorImager (Molecular Dynamics, Sunnyvale, CA).

Isolation of Mouse Parenchymal Liver Cells—10–12-week-old male C57BL/6KH mice weighing 22–27 g (Broekman Institute BV, Someren, The Netherlands) were used for parenchymal cell isolation. Hepatocytes were isolated from anesthetized mice by perfusion of the liver with collagenase (type IV, 0.05% w/v) for 10 min at 37 °C according to the method of Seglen (31). Cells were >99% pure as judged by light microscopy.

In Vitro Binding Assay—Displacement of ^{125}I-ASOR binding to mouse hepatocytes was determined as follows (32). Freshly isolated mouse parenchymal liver cells (1×10^6 cells, viability >90% as determined by 0.2% trypan blue exclusion) were incubated in 0.5 ml of Dulbecco's modified Eagle's medium (Biowhittaker, Verviers, Belgium) containing 2% BSA with 5.5 nM ^{125}I-ASOR in the presence or absence of 50 nM-5 μM displacer. After incubation for 2 h at 4 °C under gentle agitation, the medium was removed by aspiration, and the cells were washed twice with 0.2% BSA in medium and once with medium lacking BSA. Subsequently cells were counted for radioactivity. Cell binding was corrected for protein content. Nonspecific binding was measured in the presence of 100 mM GalNAc. Displacement binding data were analyzed according to a single site model using a computerized nonlinear fitting program (Prism) to calculate the K_i.

Transfection of Mouse Parenchymal Cells—The pCMV-luciferase, containing the firefly luciferase cDNA insert, was kindly provided by Crucell BV (Leiden, The Netherlands). The preparation of the K8·DNA polyplexes (N:P charge ratio 4:1; 1 μg of DNA/well in HBS buffer) was done as described by Gottschalk *et al.* (10). Mouse parenchymal liver cells were transfected 3 h after seeding (2×10^5 cells/well) with K8-condensed DNA. After a 30-min incubation of the K8·DNA complexes at room temperature, fusogenic peptides (INF7, INF7-SGSC, and INF7-K(GalNAc)$_2$) were added to a final concentration of 1–2,000 nM. After an additional incubation of 30 min at room temperature, the complexes were added directly to the parenchymal cells in 250 μl of Dulbecco's modified Eagle's medium + 0.2% BSA. After incubating for 4 h, 1 ml of medium was added, and the cells were incubated for 44 h. After harvesting of the cells the lysate was analyzed for luciferase activity as described (33) and corrected for protein content (BCA) using BSA as reference.

In analogy, BHK cells (seeded at 2×10^6 cells/well) were transfected with preformed K8·DNA condensates in the absence or presence of the fusogenic peptides.

MTT Cytotoxicity Test—Parenchymal liver cells were transfected as described above. After a 48-h incubation the medium was replaced by fresh medium, and MTT was added to a final concentration of 0.5 mg/ml. Cells were incubated for 30 min at 37 °C, the medium was removed, and dimethyl sulfoxide was added to the cells. Extinction was measured at 550 nm.

Liver Uptake and Serum Decay of INF7 and INF7-K(GalNAc)$_2$ in Mice—Male C57BL/6KH mice (19–21 g) were anesthetized, and the abdomens were opened. ^{125}I-INF7 and ^{125}I-INF7-K(GalNAc)$_2$ were injected via the inferior vena cava. At the indicated times blood samples of 50 μl were taken from the inferior vena cava and allowed to clot for 30 min. Serum samples of 10 μl were counted for radioactivity after centrifugation for 5 min at 2,500 × *g*. To determine liver uptake, liver lobules were tied off at the indicated times, excised, and weighed. At 30 min, mice were sacrificed, and organs were excised and weighed. Radioactivity in serum, liver, and other tissue samples was counted in a gamma counter (minaxi γ-counter 5000, Packard) and corrected for radioactivity in entrapped serum as described by Rensen *et al.* (28). The weight of muscle, bone, and skin was calculated from the whole body weight of the mouse and the average contribution of the organ to the body weight by the formula: % tissue in standard mouse (muscle = 22.52%, bone = 16.71%, skin = 14.74%)/100 × weight of mouse/weight of tissue sample.

RESULTS

Lytic Activity of JTS-1 and INF7—To improve the intracellular trafficking of nonviral DNA vehicles in a cell-specific fashion, we wanted to target a LDE to the ASGPr on parenchymal liver cells. In the first step, we synthesized two fusogenic peptides with known lysosome disruptive activity, JTS-1 and INF7.

The membrane-disruptive properties of JTS-1 and INF7 were determined by a liposome leakage assay, in which the release of calcein from phosphatidylcholine liposomes was measured. Liposomes with various cholesterol contents were prepared to address whether the lytic capacity of the peptides depends on the cholesterol content of the membranes. Eukaryotic plasma membranes generally contain between 20 and 25% cholesterol, whereas the cholesterol content of endosomal membranes ranges from 0 to 5% (34, 35). Cholesterol dependence is therefore an important criterion in the development of a targeted LDE because it should act specifically on endosomal membranes, leaving cell membranes unaffected.

Leakage of INF7 and JTS-1 was monitored in time at pH 5.0 and pH 7.0. Both peptides appear to be disruptive at acidic pH only (Fig. 2). In agreement with previous studies (10, 20), a kinetic study of calcein release revealed that in cholesterol-rich (40%) liposomes the INF7-induced leakage was much more rapid than that of JTS-1 ($t_{1/2}$ = 0.24 min *versus* 33.53 min, respectively; $p < 0.001$) (Fig. 3*B*). The kinetics of INF7-induced leakage of cholesterol-poor (2.6%) liposomes was found to be quite similar ($t_{1/2}$ = 0.27 min, $p < 0.01$), whereas that of JTS-1 was accelerated considerably compared with that of cholesterol-rich liposomes ($t_{1/2}$ = 4.9 min) (Fig. 3*C*). Moreover JTS-1 induced partial leakage of liposomes containing 2.6% cholesterol (Fig. 3*C*).

Further study confirmed the differential cholesterol dependence of JTS-1- and INF7-induced lysis. Whereas INF7 was equally fusogenic in liposomes with high and low cholesterol content, JTS-1 was only able to disrupt cholesterol-rich liposomes completely (Fig. 3*A*).

From these results we concluded that INF7 caused a rapid, cholesterol-independent disruption with an EC_{50} of ~1.3 μM, whereas JTS-1-induced leakage is much slower and cholesterol-dependent. Given that the lysosomal membrane is cholesterol-poor, we selected INF7 for subsequent design of a targeted fusogenic peptide, by conjugation to the -K(GalNAc)$_2$ ligand (Fig. 1).

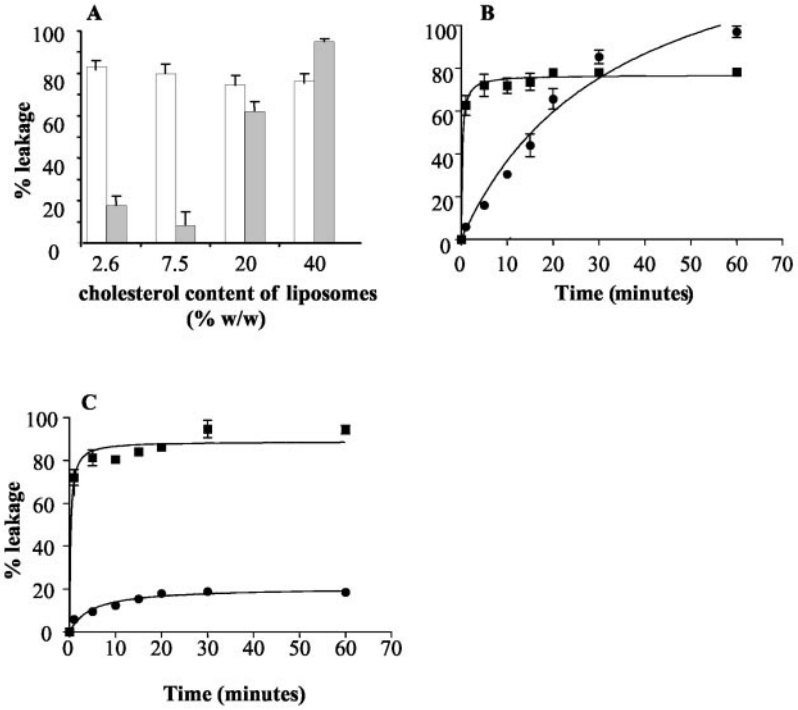

FIG. 3. **Liposome leakage assay of INF7 and JTS-1.** Calcein-containing liposomes were incubated with 10 μM peptide at pH 5.0. Calcein release was quantified as described under "Experimental Procedures." *A*, calcein leakage from liposomes containing 2.6–40% w/w cholesterol after incubation with INF7 (*empty bars*) or JTS-1 (*gray bars*). *B*, kinetics of JTS1- (●) and INF7- (■) induced calcein leakage from 40% w/w cholesterol liposomes. *C*, kinetics of JTS1- (●) and INF7- (■) induced calcein leakage from 2.6% w/w cholesterol liposomes. Data are the means ± S.D. of a determination in triplicate.

In Vitro Binding Studies—The affinity of INF7-K(GalNAc)$_2$ for the ASGPr was monitored by an *in vitro* competition assay of ^{125}I-ASOR total binding to mouse parenchymal liver cells. As shown in Fig. 4, INF7-K(GalNAc)$_2$ inhibited the binding of ASOR to the ASGPr (K_d 87 nM), which is comparable with that of K(GalNAc)$_2$ (K_d 32 nM). We previously used the K(GalNAc)$_2$ with comparable affinity (32, 41). This indicates that attachment of the INF7 peptide to K(GalNAc)$_2$ did not affect the affinity of K(GalNAc)$_2$ for the ASGPr considerably. To exclude nonspecific binding caused by the presence of the SGSC linker arm between the GalNAc cluster and the peptide, an INF7-SGSC was synthesized and tested for the affinity of the ASGPr. INF7 and INF7-SGSC, the peptide with the SGSC linker arm between the peptide and GalNAc, did not show any affinity for the ASGPr (Fig. 4), confirming the importance of K(GalNAc)$_2$ in the binding to ASGPr.

Lytic Activity of INF7 and the INF7 Glycoconjugate—The membrane-disruptive potency of INF7-K(GalNAc)$_2$ was determined in the liposome leakage assay, similar to INF7 and JTS-1. INF7-K(GalNAc)$_2$ displayed only lytic activity at acidic pH (data not shown). The leakage kinetics of INF7-K(GalNAc)$_2$ were comparable with that of INF7 (Fig. 5). In cholesterol-poor (2.6%) liposomes, the fusogenic capacity of the glycoconjugate appeared to be five times lower than that of the parental INF7 (Fig. 5*B*) (EC_{50} 1.3 and 6.1 μM, respectively). A closer look at the cholesterol dependence of liposome leakage showed that the fusogenic activity of INF7-K(GalNAc)$_2$ was impaired markedly in liposomes with cholesterol contents above 20% (Fig. 5*C*). When aiming at lysosome-specific membrane disruption, this is a clear advantage because lysosomal membranes are known to contain low cholesterol concentrations, whereas plasma membranes are generally rich in cholesterol. This implies that INF7-K(GalNAc)$_2$ may be even more specific for lysosomal membranes, while leaving the cell membrane intact.

Mechanism of Leakage—We argued that the differential capacity of INF7 and INF7-K(GalNAc)$_2$ to lyse cholesterol-rich membranes might be related to the actual mechanism of membrane disruption. Previous studies have shown that amphipathic peptides are disruptive either by facilitating pore formation after multimeric assembly of the peptide or by inducing a more detergent-like solubilization of the liposome leading to complete disruption of the liposome. It was reasoned that pore formation might restrict the leakage of entrapped compounds with a low molecular weight, whereas the molecular weight of entrapped compounds would not be a limiting factor after complete disruption of the liposomes (36). For that reason we studied the size-dependent leakage of INF7 and INF7-K(GalNAc)$_2$ in liposomes containing either calcein (molecular weight, 622) or ^{125}I-trypsin inhibitor (molecular weight, 20,000). Liposomes were incubated with INF7 or INF7-K(GalNAc)$_2$ (0–20 μM). At pH 7.0, no leakage of calcein or trypsin was observed for up to 60 min of incubation. However, under acidic conditions, INF7 and INF7-K(GalNAc)$_2$ promoted the release of calcein but not of entrapped ^{125}I-trypsin inhibitor (Fig. 6). This suggests that the observed leakage caused by INF7 and INF7-K(GalNAc)$_2$) is likely caused by pore formation.

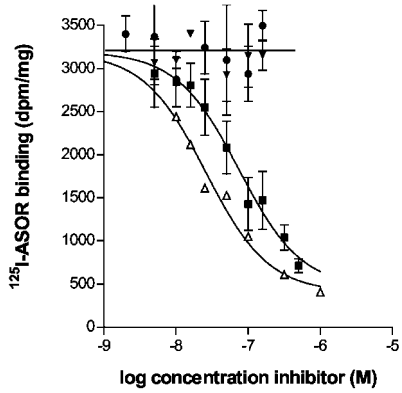

FIG. 4. **Competition of ^{125}I-ASOR binding to mouse parenchymal liver cells by INF7 (▼), INF7-SGSC (●), INF7-K(GalNAc)$_2$ (■), and K(GalNAc)$_2$ (△).** Parenchymal liver cells (1×10^6) were incubated for 2 h at 4 °C with 5.5 nM ^{125}I-ASOR in the presence or absence of 0.005–5 μM INF7-K(GalNAc)$_2$. Data were analyzed according to a single site model using a computerized nonlinear-fitting program (Prism 3.0). The affinity of INF7-K(GalNAc)$_2$ was calculated to be 87 ± 16 nM compared with 32 ± 9 nM. Values are the means ± S.D. of two determinations in triplicate.

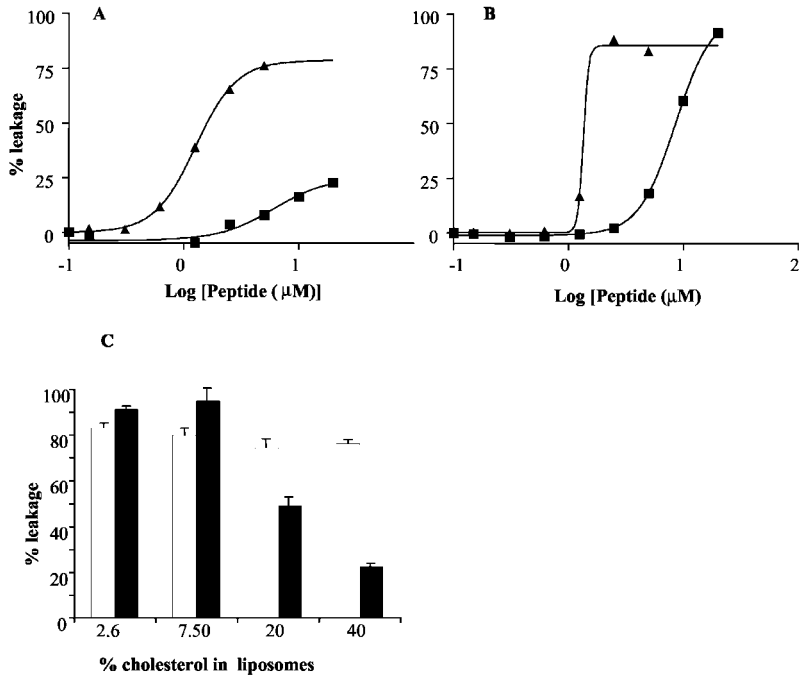

FIG. 5. **Liposome leakage assay of INF7 and INF7-K(GalNAc)$_2$.** Calcein release was quantified as described under "Experimental Procedures." *A*, calcein-laden 40% cholesterol liposomes were incubated at pH 5 with 0–20 μM INF7 (▲) or INF7-K(GalNAc)$_2$ (■). After 30 min of incubation calcein leakage was measured and is plotted as a percent of total entrapped calcein. *B*, calcein-laden 2.6% cholesterol liposomes were incubated at pH 5.0 with 0–20 μM INF7 (▲) or INF7-K(GalNAc)$_2$ (■). *C*, calcein leakage from liposomes containing 2.6–40% cholesterol after incubation with 10 μM peptide at pH 5.0. Indicated are the percentages of calcein leakage from liposomes containing various cholesterol concentrations incubated with INF7 (*empty bars*) or INF7-K(GalNAc)$_2$ (*solid bars*). Data are the means ± S.D. of a determination in triplicate.

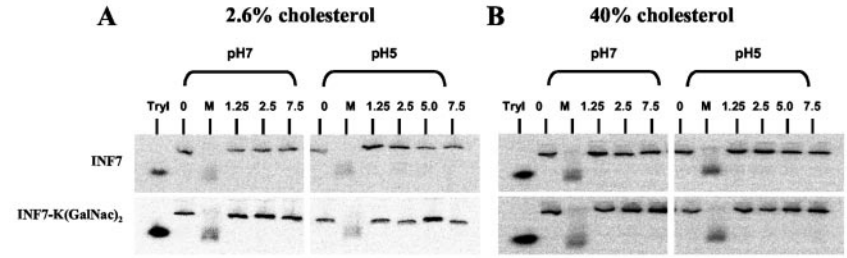

FIG. 6. **Liposome leakage of INF7 and INF7-K(GalNAc)$_2$.** Release of ^{125}I-trypsin inhibitor from 2.6% cholesterol (*A*) or 40% cholesterol (*B*) liposomes after incubation for 30 min at pH 5.0 and 7.0 in the presence of peptide (0–7.5 μM). As a measure of total liposome leakage, liposomes were incubated with 0.2% Triton X-100 (*lane M*). Release of liposome-incorporated ^{125}I-trypsin inhibitor (*TryI*) was visualized after agarose gel electrophoresis and subsequent autoradiography with a PhosphorImager. After quantification of the intensity of the bands no significant INF7- and INF7-K(GalNAc)$_2$-induced leakage was observed.

Effect of the Fusogenic Peptides on Polyplex Gene Transfer to Mouse Parenchymal Liver Cells—Next, we assessed whether the glycoconjugated INF7 was able to promote the release of lysosomally entrapped DNA to the cytosol, thus enhancing the transfection level in a receptor-dependent manner. Mouse parenchymal liver cells were transfected with polyplexed DNA in the absence or presence of fusogenic peptide. For gene transfer we made use of the cationic peptide (K8)-based polyplex protocol described by Gottschalk *et al.* (10). Cells were transfected with plasmid DNA (pCMVLuc), containing a CMV promoter-driven luciferase reporter gene insert, which was condensed with K8 (at a N:P ratio of 4:1). To exclude artifacts caused by the presence of the SGSC linker arm between the GalNAc cluster and the peptide, INF7-SGSC was included as a control. Preincubation of the polyplexes with INF7 increased the transfection efficiency in a dose-dependent manner up to 30-fold (Fig. 7*A*). At the concentrations measured, INF-K(GalNAc)$_2$ displayed a capacity to enhance the transfection efficiency similar to that of INF7.

Receptor-specific Recognition of INF7-K(GalNAc)$_2$—INF7-K(GalNAc)$_2$ was not able to stimulate gene transfer to BHK cells, which do not express the ASGPr, whereas INF7 and INF7-SGSC were found to improve the transfection efficiency of the K8 polyplexes considerably (Fig. 7*B*).

To confirm that INF7-K(GalNAc)$_2$ promoted nonviral gene transfer of K8·DNA in an ASGPr-specific fashion, the effect of INF7-K(GalNAc)$_2$ on the transfection efficiency was examined in the presence of GalNAc, which blocks the ASGPr. As shown in Fig. 7*C*, GalNAc did not influence the transfection ability of polyplexes that were preincubated with INF7 or INF7-SGSC, whereas it markedly reduced that of INF7-K(GalNAc)$_2$-preincubated polyplexes. GlcNAc, which has no affinity for the ASGPr, by contrast, had no effect on INF7-K(GalNAc)$_2$-stimulated gene transfer. This indicates that INF7-K(GalNAc)$_2$ exerts its fusogenic activity through the ASGPr, whereas INF7 has a more general nonspecific fusogenic effect.

Toxicity—It has been suggested that disruption of endocytotic and lysosomal vesicles might lead to the release of pro-apoptotic and cytotoxic proteases. Therefore, we mapped the toxic side effects of the targeted LDEs by evaluating the effect of INF7 or glycoconjugated INF7, in the presence of the K8·DNA polyplexes, on the viability of parenchymal liver cells. INF7 and INF7-K(GalNAc)$_2$-equipped polyplexes did not show significant toxicity in the applied relevant concentration range (0–2 μM) (data not shown).

In Vivo Behavior of INF7 and INF7-K(GalNAc)$_2$ in Mice—To study the biodistribution profile of INF7 and INF7-K(GalNAc)$_2$ in mice, both peptides were iodinated and intravenously injected into the vena cava of C57BL/6 mice. INF7 was cleared rapidly from the circulation at a half-life of ~2 min (Fig. 8*B*), and only 5% of the injected dose could be recovered in the liver after 30 min (Fig. 8*A*). Fig. 8*C* shows that hepatic uptake of

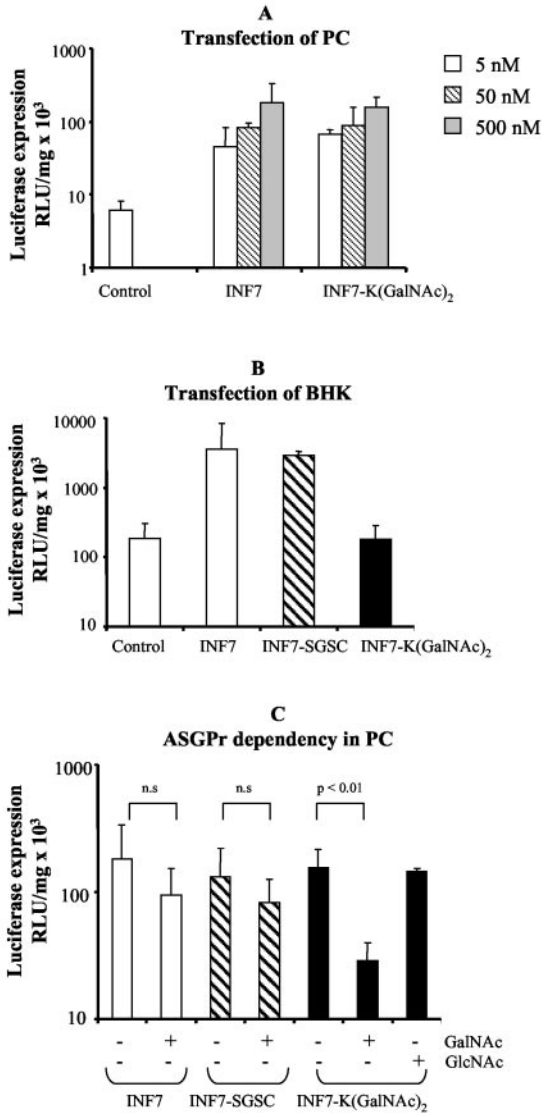

FIG. 7. **Effect of INF7, INF7-SGSC, and INF7-K(GalNAc)$_2$ on nonviral gene transfer to mouse parenchymal liver cells (*A*) or 500 nM BHK cells (*B*).** Plasmid DNA (1 μg/well pCMVLuc) was condensed in HBS with K8 peptide at a 4:1 P:N ratio, polyplexes were incubated in the absence (*dotted bar*) or presence of INF7 (*empty bar*), INF7-SGSC (*hatched bar*), and INF7-K(GalNAc)$_2$ (*solid bar*). *C* shows the effect of 100 mM GalNAc and 100 mM GlcNAc on nonviral gene transfer in the presence of (targeted) LDEs in mouse parenchymal cells. Data are the means ± S.D. of four determinations in triplicate.

INF7 is ~5%, which was comparable with skin, bone, kidney, and intestine. INF7-K(GalNAc)$_2$ was cleared even more rapidly from the circulation (half-life <2 min, Fig. 8*B*). In contrast to INF7, the glycoconjugate was taken up mainly by the liver (35–40%; Fig. 8, *A* and *C*), whereas uptake by small intestine, kidney, and bone was significantly lower. This comparison of the INF7 and INF7-K(GalNAc)$_2$ biodistribution profiles indicates that attachment of the K(GalNAc)$_2$ group to INF7 specifically redirects INF7 to the liver.

DISCUSSION

The main objective of this study was to improve nonviral gene delivery by the use of targeted LDEs. As a first step we have tested two HA-derived fusogenic peptides, JTS-1 and INF7, for their lysosome disruptive capacity in calcein-laden liposomes (10). INF7 was found to induce a rapid and cholesterol-independent leakage of liposomes, whereas JTS-1-induced leakage was much slower and cholesterol-dependent.

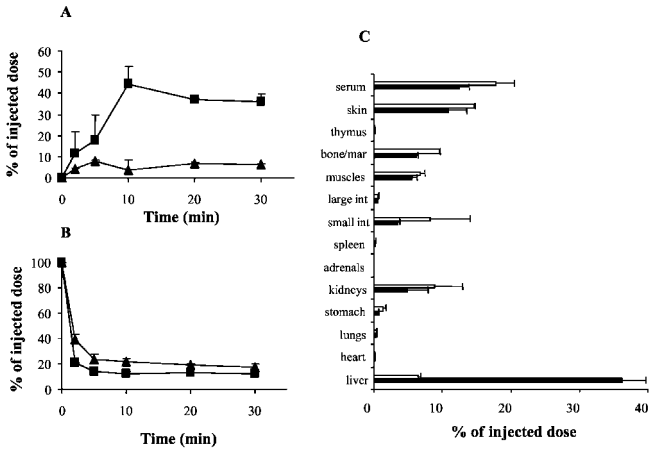

FIG. 8. Liver uptake (*A*) and serum decay (*B*) of INF7 (▲) and INF7-K(GalNAc)$_2$ (■) in mice. Compounds (25 μg) were injected intravenously, blood and liver samples were taken at indicated time points, and radioactivity was determined. Values were plotted as percentage of the injected dose. Liver and organ uptakes are corrected for radioactivity in entrapped serum. *C*, organ distribution of ^{125}I-INF7 (*empty bars*) and ^{125}I-INF7-K(GalNAc)$_2$ (*solid bars*). 30 min after the intravenous injection of the compounds, mice were sacrificed, and organs were excised and analyzed for associated radioactivity. Values are the means ± S.D. of two experiments.

Moreover, JTS-1 was unable to disrupt cholesterol-poor (<20%) liposomes completely. These findings concur with the studies of Gottschalk *et al.* (10), who showed complete leakage of cholesterol-poor liposomes by INF7 compared with only partial leakage by JTS-1 (35%). The differential fusogenic profile of JTS-1 and INF7 is not the result of differences in net negative charge or hydrophobicity of the peptides because the peptides are very similar in that respect. Possibly, INF7 and JTS-1 have a different orientation in liposomal membranes (12, 37–40). Further experiments will be imperative to confirm this hypothesis.

In the second step, the most promising peptide, INF-7, was equipped with a homing device to render the peptide specific for parenchymal liver cells. As a homing device we used K(GalNAc)$_2$, which was shown previously to be able to redirect liposomes, lipoproteins, and drugs to liver parenchymal cells (26, 32, 41). The conjugate appeared to be slightly less fusogenic than the parent peptide (1.3 μM *versus* 6.1 μM). However, the lytic activity of the conjugate was cholesterol-dependent in that it only disrupted cholesterol-poor liposomes. This may be an advantage as K(GalNAc)$_2$-conjugated INF7 is designed to act specifically on the cholesterol-deficient lysosomal membranes of ASGPr-expressing cells. INF7, by contrast, may also be fusogenic at the level of the plasma membrane.

The intriguing observation that INF7-K(GalNAc)$_2$-induced leakage depends on the liposome cholesterol content, in contrast to INF7 alone, prompted further study. Lysosome disruptive peptides may facilitate leakage, through pore formation and through a detergent-like solubilization of the membrane (36). The differential lytic profile of INF7 and its glycoconjugate suggests that INF7 disrupts membranes via both pathways, one of which predominates in cholesterol-rich membranes and is blocked by the presence of the bulky glycoside moiety. However, the lack of leakage of ^{125}I-trypsin inhibitor from INF7 (glycoconjugate)-treated liposomes points to pore formation as the major pathway of liposome disruption for both INF7 and the glycoconjugated INF7. Rather, steric hindrance of the exposed glycoside group might interfere with the ability of the fusogenic peptide to form pores. This also explains the reduced lytic activity of INF7-K(GalNAc)$_2$ in cholesterol-rich liposomes because the liposomal cholesterol may hamper pore formation by INF7-K(GalNAc)$_2$ caused by steric hindrance of the glyco-

side group. To confirm this hypothesis, the orientation and distribution of the peptides in the liposomal membrane need to be addressed.

The glycoconjugated peptide was designed for ASGPr-directed delivery. Indeed, glycoconjugated INF7 bound to the ASGPr with an affinity of 87 nM, which is about two times lower than $K(GalNAc)_2$ itself. Earlier studies have shown that an affinity of 87 nM for the ASGPr should be sufficient for effective targeting of INF7-$K(GalNAc)_2$ (32, 42).

The final goal of this study was to elaborate a targeted LDE for improving nonviral gene transfer. To this end, we have evaluated the effect of the fusogenic peptides on the gene transfer efficiency of an established nonviral gene delivery protocol based on the cationic peptide K8 in mouse parenchymal liver cells (10). DNA polyplexed with small sized synthetic oligocations (like K8) may be better for systemic application because the derived condensates generally are smaller and less immunogenic, nonaggregating, and are readily unpacked intracellularly (43, 44). INF7, INF7-SGSC, and INF7-$K(GalNAc)_2$ led to a substantial, 30-fold, increase in the transfection efficiency of K8·DNA complexes in freshly isolated parenchymal cells. This stimulatory effect was concentration-dependent. Even though in the leakage assay, INF7-$K(GalNAc)_2$ appeared to be 6-fold less potent than INF7, the lower intrinsic activity is compensated for by the enhanced uptake of the targeted peptide, by parenchymal liver cells. However, it should also be kept in mind that liposomal and cellular assays are not fully comparable.

The fusogenic activity of INF7-$K(GalNAc)_2$ was abolished completely in the presence of excess GalNAc, which blocks ASGPr-mediated uptake, whereas GlcNAc had no effect on the transfection efficiency. Moreover, INF7-$K(GalNAc)_2$ did not affect the transfection yield in ASGPr-deficient BHK cells, whereas INF7 and INF7-SGSC were equally potent in BHK and mouse parenchymal cells. This underlines that the stimulatory effect of glycoconjugated INF7 is mediated by the ASGPr and will have fewer side effects. In agreement with previous studies, primary parenchymal liver cells are more difficult to transfect than continuous cell lines; the intrinsic transfection efficacy in BHK cells was indeed found to be 10–100-fold higher than in parenchymal cells (45).

The observation that INF7-$K(GalNAc)_2$ was completely inactive in BHK cells indicates that non-ASGPr-mediated uptake and the lytic activity of INF7-$K(GalNAc)_2$ are reduced considerably compared with those of INF7 or INF7-SGSC. As our leakage data already showed that the glycoconjugate is less fusogenic, we propose that this is the major contributing factor underlying the reduced stimulatory effect of INF7-$K(GalNAc)_2$ in BHK cells. The actual route of entry of INF7 and INF7-SGSC remains unclear. INF7 and INF7-SGSC may be cointernalized into the target cells, associated with the polyplexes. Because the peptides have only a very weak fusogenic activity at pH 7.4, it is unlikely that they may be stimulatory by facilitating polyplex/plasma membrane fusion. Cellular uptake of the cationic polyplexes may in turn implicate the use of receptor systems, possibly the scavenger receptor class B and CD36 (46), or alternative pathways such as pinocytosis. INF7-$K(GalNAc)_2$, on the other hand, could be stimulatory by associating with the K8·DNA complex and subsequently promoting whole complex uptake via an ASGPr-mediated pathway. Intracellularly, INF7-$K(GalNAc)_2$ will promote escape of the DNA from the lysosomal compartment.

It has been reported that lysosome leakage and membrane disruption may lead to intracellular release of lytic enzymes including proteases, nucleases, and lipases. Although these enzymes are acid hydrolases, with a catalytic optimum near pH 5.0, leakage of these enzymes in the cytoplasm of the cell could promote apoptosis or necrosis (47). We show that the peptides are not cytotoxic in parenchymal liver cells.

Another important issue in regard of potential *in vivo* use involves the pharmacokinetics of INF7 and its glycoconjugate. The biodistribution profile in mice shows that INF7-$K(GalNAc)_2$ is preferentially taken up by the liver, whereas INF7 is distributed evenly over various organs. In fact, liver uptake of the glycoconjugate is 6-fold higher than that of INF7, indicating that we have developed a hepatocyte-specific LDE for use *in vivo*.

In conclusion, we present a targeted fusogenic peptide, INF7-$K(GalNAc)_2$, which induces lysosomal escape in a receptor-dependent fashion. Its favorable pH- and cholesterol-dependent activity profile makes it even more lysosome-specific than the parental INF7. We envision that INF7-$K(GalNAc)_2$ could be applied to improve the transfection efficacy of hepatic nonviral gene transfer vehicles (25) and of antisense drugs for hepatic genes (42, 41, 48) by facilitating the escape from the lysosomal pathway, which appears to be a major drawback in both therapies (49). Not only gene medicines, but also other drugs that accumulate in the lysosomal circuit might benefit from application of targeted LDEs.

REFERENCES

1. Niidome, T., Urakawa, M., Sato, H., Takahara, Y., Anai, T., Hatakayama, T., Wada, A., Hirayama, T., and Aoyagi, H. (2000) *Biomaterials* **21,** 1811–1819
2. Kichler, A., Mechtler, K., Behr, J. P., and Wagner, E. (1997) *Bioconj. Chem* **8,** 213–221
3. Simoes, S., Slepushkin, V., Pires, P., Gaspar, R., de Lima, M. C. P., and Duzgunes, N. (1999) *Gene Ther.* **65,** 1798–1807
4. Watabe, A., Yamaguchi, T., Kawanishi, T., Uchida, E., Eguchi, A., Mizuguchi, H., Mayumi, T., Nakanishi, M., and Hayakawa, T. (1999) *Biochim. Biophys. Acta Biomembr.* **12,** 1–2
5. Zanta, M. A., Belguise Valladier, P., and Behr, J. P. (1999) *Proc. Natl. Acad. Sci. U. S. A.* **96,** 91–96
6. Lim, D. W., Yeom, Y. I., and Park, T. G. (2000) *Bioconj. Chem.* **11,** 688–695
7. Morris, M. C., Vidal, P., Chaloin, L., Heitz, F., and Divita, G. (1997) *Nucleic Acids Res.* **25,** 2730–2736
8. Torchilin, V. P., Rammohan, R., Weissig, V., and Levchenko, T. S. (2001) *Proc. Natl. Acad. Sci. U. S. A.* **98,** 8786–8791
9. Wolfert, M. A., and Seymour, L. W. (1998) *Gene Ther.* **5,** 409–414
10. Gottschalk, S., Sparrow, J. T., Hauer, J., Mims, M. P., Leland, F. E., Woo, S. L. C., and Smith, L. C. (1996) *Gene Ther.* **3,** 448–457
11. Wyman, T. B., Nicol, F., Zelphati, O., Scaria, P. V., Plank, C., and Szoka, F. C. (1997) *Biochemistry* **36,** 3008–3017
12. Martin, I., Pecheur, E. I., Ruysschaert, J. M., and Hoekstra, D. (1999) *Biochemistry* **38,** 9337–9347
13. Chowdhury, N. R., Hays, R. M., Bommineni, V. R., Franki, N., Chowdhury, J. R., Wu, C. H., and Wu, G. Y. (1996) *J. Biol. Chem.* **271,** 2341–2346
14. Plourde, R., Phillips, A. T., Wu, C. H., Hays, R. M., Chowdhury, J. R., Chowdhury, N. R., and Wu, G. Y. (1996) *Bioconj. Chem.* **7,** 131–137
15. Arar, K., Aubertin, A. M., Roche, A. C., Monsigny, M., and Mayer, R. (1995) *Bioconj. Chem.* **6,** 573–577
16. Derossi, D., Chassaing, G., and Prochiantz, A. (1998) *Trends Cell Biol.* **8,** 84–87
17. Schoen, P., Chonn, A., Cullis, P. R., Wilschut, J., and Scherrer, P. (1999) *Gene Ther.* **6,** 823–832
18. Decout, A., Labeur, C., Goethals, M., Brasseur, R., Vandekerckhove, J., and Rosseneu, M. (1998) *Biochim. Biophys. Biomembr.* **1372,** 102–116
19. Plank, C., Oberhauser, B., Mechtler, K., Koch, C., and Wagner, E. (1994) *J. Biol. Chem.* **269,** 12918–12924
20. Wagner, E., Plank, C., Zatloukal, K., Cotten, M., and Birnstiel, M. L. (1992) *Proc. Natl. Acad. Sci. U. S. A.* **89,** 7934–7938
21. Smith, L. C., Duguid, J., Wadhwa, M. S., Logan, M. J., Tung, C. H., Edwards, V., and Sparrow, J. T. (1998) *Adv. Drug Del. Rev.* **30,** 115–131
22. Vaysse, L., Burgelin, I., Merlio, J. P., and Arveiler, B. (2000) *Biochim. Biophys. Acta* **26,** 369–376
23. Zhang, X., Simmons, C. G., and Corey, D. R. (2001) *Bioorg. Med. Chem. Lett.* **11,** 1269–1272
24. Sliedregt, L., Rensen, P. C. N., Rump, E. T., van Santbrink, P. J., Bijsterbosch, M. K., Valentijn, A., van der Marel, G. A., van Boom, J. H., van Berkel, T. J. C., and Biessen, E. A. L. (1999) *J. Med. Chem.* **42,** 609–618
25. Nishikawa, M., Yamauchi, M., Morimoto, K., Ishida, E., Takakura, Y., and Hashida, M. (2000) *Gene Ther.* **7,** 548–555
26. Valentijn, R. A., van der Marel, G. A., Sliedregt, L. A. J. M., van Berkel, T. J. C., Biessen, E. A. L., and van Boom, J. H. (1997) *Tetrahedron* **53,** 759–770
27. Huang, H., and Rabenstein, D. L. (1999) *J. Pept. Res.* **53,** 548–553
28. Rensen, P. C. N., Schiffelers, R. M., Versluis, A. J., Bijsterbosch, M. K., VanKuijkMeuwissen, M., and van Berkel, T. J. C. (1997) *Mol. Pharmacol.* **52,** 445–455
29. McFarlane, A. S. (1958) *Nature* **182,** 53–58
30. Redgrave, T. G., Roberts, D. C. K., and West, C. E. (1975) *Anal. Biochem.* **65,**

42–49
31. Seglen, P. O. (1976) *Methods Cell Biol.* **13,** 29–83
32. Rensen, P. C. N., Sliedregt, L., Ferns, A., Kieviet, E., van Rossenberg, S. M. W., van Leeuwen, S. H., van Berkel, T. J. C., and Biessen, E. A. L. (2001) *J. Biol. Chem.* **276,** 37577–37584
33. Cotten, M., Wagner, E., and Birnstiel, M. L. (1993) *Methods Enzymol.* **217,** 618–644
34. Kobayashi, T., Yamaji Hasegawa, A., and Kiyokawa, E. (2001) *Semin. Cell Dev. Biol.* **12,** 173–182
35. Alberts, B., Bray, D., Lewis, J., Raff, M., Roberts, K., and Watson, J. D. (1983) *Molecular Biology of the Cell*, p. 260, Garland Publishing, Inc., New York
36. Parente, R. A., Nir, S., and Szoka, F. C., Jr. (1990) *Biochemistry* **29,** 8720–8728
37. Pecheur, E. I., Martin, I., Ruysschaert, J. M., Bienvenue, A., and Hoekstra, D. (1998) *Biochemistry* **37,** 2361–2371
38. Pecheur, E. I., Sainte Marie, J., Bienvenue, A., and Hoekstra, D. (1999) *Biochemistry* **38,** 364–373
39. Pecheur, E. I., Sainte Marie, J., Bienvenue, A., and Hoekstra, D. (1999) *J. Membr. Biol.* **167,** 1–17
40. Pecheur, E. I., Martin, I., Bienvenue, A., Ruysschaert, J. M., and Hoekstra, D. (2000) *J. Biol. Chem.* **275,** 3936–3942
41. Biessen, E. A. L., Sliedregt-Bol, K. M., 'T Hoen, P. A., Prince, P., Van der Bilt, E., Valentijn, A. R., Meeuwenoord, N. J., Princen, H., Bijsterbosch, M. K., Van der Marel, G. A., Van Boom, J. H., and van Berkel, T. J. (2002) *Bioconj. Chem.* **13,** 295–302
42. Biessen, E. A. L., Vietsch, H., Rump, E. T., Fluiter, K., Kuiper, J., Bijsterbosch, M. K., and van Berkel, T. J. C. (1999) *Biochem. J.* **3,** 783–792
43. McKenzie, D. L., Collard, W. T., and Rice, K. G. (1999) *J. Pept. Res.* **54,** 311–318
44. Wadhwa, M. S., Collard, W. T., Adami, R. C., McKenzie, D. L., and Rice, K. G. (1997) *Bioconj. Chem.* **8,** 81–88
45. Beck, N. B., Sidhu, J. S., and Omiecinski, C. J. (2000) *Gene Ther.* **7,** 1274–1283
46. Terpstra, V., van Amersfoort, E. S., van Velzen, A. G., Kuiper, J., and van Berkel, T. J. C. (2000) *Arterioscler. Thromb. Vasc. Biol.* **20,** 1860–1872
47. Zang, Y., Beard, R. L., Chandraratna, R. A. S., and Kang, J. X. (2001) *Cell Death Differ.* **8,** 477–485
48. Sugano, M., and Makino, N. (1996) *J. Biol. Chem.* **271,** 19080–19083
49. Akhtar, S., Hughes, M. D., Khan, A., Bibby, M., Hussain, M., Nawaz, Q., Double, J., and Sayyed, P. (2000) *Adv. Drug Del. Rev.* **44,** 3–21

Targeted Lysosome Disruptive Elements for Improvement of Parenchymal Liver Cell-specific Gene Delivery

Sabine M. W. van Rossenberg, Karen M. Sliedregt-Bol, Nico J. Meeuwenoord, Theo J. C. van Berkel, Jacques H. van Boom, Gijs A. van der Marel and Erik A. L. Biessen

J. Biol. Chem. 2002, 277:45803-45810.
doi: 10.1074/jbc.M203510200 originally published online September 16, 2002
